

# Hybrid Ionogel Electrolytes Derived from Polyhedral Oligomeric Silsesquioxane for Lithium Ion Batteries

Jin Hong Lee<sup>1,2,†</sup>, Albert S. Lee<sup>1,3,†</sup>, Jong-Chan Lee<sup>2</sup>, Soon Man Hong<sup>1,3</sup>,  
Seung Sang Hwang<sup>1,3</sup>, and Chong Min Koo<sup>1,3,\*</sup>

<sup>1</sup>Materials Architecturing Research Center, Korea Institute of Science and Technology, Seoul 136-791, Republic of Korea

<sup>2</sup>Department of Chemical and Biological Engineering, Seoul National University, Seoul 151-744, Republic of Korea

<sup>3</sup>Nanomaterials Science and Engineering, University of Science and Technology, Daejeon 305-333, Republic of Korea

Inorganic–organic hybrid ionogels fabricated with 1 M LiTFSI in *N*-butyl-*N*-methylpyrrolidinium bis(trifluoromethylsulfonyl)imide (BMPTFSI) crosslinked with a fully methacryl-substituted Polyhedral Oligomeric Silsesquioxane (T8-MMA-POSS) were investigated as gel polymer electrolytes for lithium ion batteries. The effect of T8-MMA-POSS on physical properties of the ionogels was characterized in terms of dimensional stability, ion transport behaviour, and thermal stability. A mere 5 wt% concentration of the cross-linker was able to produce non-flowing hybrid ionogels, leading to high ionic conductivity with good mechanical properties. The lithium battery cell fabricated with ionogels revealed high specific capacity and excellent cycling performance with high Coulombic efficiency at elevated temperature, demonstrating that hybrid ionogels could be a promising candidate electrolyte for use in lithium ion batteries.

**Keywords:** Silsesquioxane, Ionic Liquids, Lithium Ion Batteries, Gel Polymer Electrolytes.

## 1. INTRODUCTION

Inorganic–organic hybrid electrolytes, such as sol–gel based solid polymer electrolytes and solidified ionic liquid ionogels, have been a hot topic of materials scientists for various electrochemical applications, including electrochromic devices, capacitors, and lithium ion batteries, because of their good thermal and electrochemical stabilities, and mechanical robustness.<sup>1–4</sup> However, the challenges of utilizing these sol–gel derived hybrid materials are the electrochemical instability of uncondensed silanol groups from uncontrolled siloxane structure, thus requiring substantial thermal treatments at elevated temperature.<sup>2</sup>

Polyhedral Oligomeric Silsesquioxanes, or more commonly known as POSS, are inorganic–organic hybrid materials with well-defined, inorganic siloxane polyhedral cores, with covalently bound organic functional groups stemming radially outwards.<sup>5</sup> The inner inorganic core is known as the smallest silica particle, as the free-volume of the POSS was reported to be as small as a sphere

with diameter  $\sim 3$  nm.<sup>5</sup> This nano-sized core and organic functional groups allows for solubility and/or impeccable dispersability in a wide variety of solvents. Moreover, through the myriad of organic functional groups that can be introduced, various functional materials can be fabricated through thermal or UV-initiated processes.<sup>6,7</sup>

The use of POSS-based materials for fabrication of hybrid electrolytes has been predominately been reported for solid polymer electrolytes. Various polymer chemistries,<sup>8</sup> as well as blend composites<sup>9</sup> have employed for the manipulation of hybrid electrolytes for lithium ion batteries. However, solid polymer electrolytes still suffer from relatively low ionic conductivity, hampering their use in real-life settings.

In this study, we fabricated a hybrid ionogel with a fully methacryl-substituted POSS (T8-MMA-POSS). At a low T8-MMA-POSS concentration of 5 wt%, the ionic liquid is fully solidified with non-leaking property. Examination of various properties including compatibility with ionic liquids, thermal, mechanical, and electrochemical traits reveal that these hybrid ionogels are highly promising materials for next generation hybrid ionogel electrolytes.

\*Author to whom correspondence should be addressed.

†These two authors contributed equally to this work.

## 2. EXPERIMENTAL DETAILS

### 2.1. Synthesis of *N*-butyl-*N*-methylpyrrolidinium bis(trifluoromethylsulfonyl)imide

Synthesis of *N*-butyl-*N*-methylpyrrolidinium bis(trifluoromethylsulfonyl)imide was performed following literature procedure.<sup>11,12</sup> In a dry 500 mL round-bottom flask, stoichiometric amounts of 1-methylpyrrolidine (50 g, 0.59 mol) and 1-iodobutane (108 g, 0.59 mol) in 250 mL of ethyl acetate were magnetically stirred at room temperature for 24 h. The product was repeatedly washed with ethyl acetate and filtered until pure white salt of BMPI was obtained. BMPI was then dissolved in deionized water and mixed with a stoichiometric amount of LiTFSI dissolved in deionized water. The organic phase was extracted with methylene chloride and subsequently dried at 100 °C for 24 h to remove any residual water. The resulting BMP-TFSI had H<sub>2</sub>O content of less than 100 ppm as measured with the Karl Fischer method. Ionic liquid solutions of 1 M LiTFSI in *N*-butyl-*N*-methylpyrrolidinium bis(trifluoromethylsulfonyl)imide (BMPTFSI) were made by dissolving LiTFSI at 60 °C for 24 hours and drying at 100 °C overnight prior to use.

### 2.2. Preparation of Hybrid Ionogels

T8-MMA-POSS (Fig. 1) was purchased from Hybrid Plastics and used as received. In an inert, argon-charged glove, solutions with various amounts of T8-MMA-POSS in BMPTFSI were prepared in glass vial. An amount of 1 wt% (relative to T8-MMA-POSS) of AIBN as thermal initiator was added to this solution. After taking the solutions out of the glove box, samples were sonicated and shaken for 10 min or until the solution was homogenous. Then, the samples were directly taken to an oven preset at 70 °C for 3 h.<sup>12</sup> The hybrid ionogel electrolytes were named as HIE-5 and HIE-10 for ionogels containing 5 and 10 wt% of T8-MMA-POSS, respectively.

### 2.3. Characterizations and Measurements

Fourier transform infrared spectra were measured with a Perkin-Elmer FT-IR system Spectrum-GX. Thermal gravimetric analysis was carried out with TA instrument

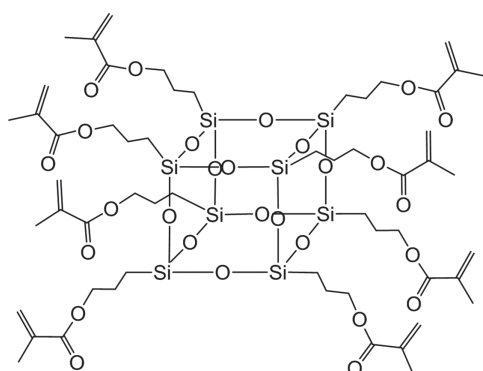


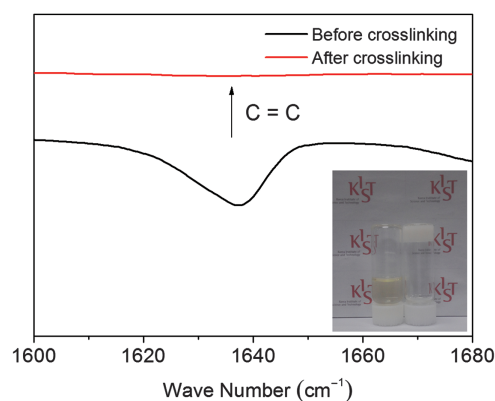
**Figure 1.** Chemical structure of T8-MMA-POSS.

(TGA 2950) at heating rate of 10 °C min<sup>-1</sup> under N<sub>2</sub> atmosphere. Rheological properties were examined using a rheometer (Advanced Rheometric Expansion System, ARES) instrument with cone-plate geometry (25 mm diameter). All rheological measurements were performed in the linear viscoelastic region under N<sub>2</sub> atmosphere. The ionic conductivity was determined using a complex impedance analyzer (Bio-Logics, VMP3) over frequency range from 1 Hz to 1 MHz at AC amplitude of 10 mV. The electrochemical stability of the gel polymer electrolytes was examined using a linear sweep voltammetry system. In the experiments, a stainless steel working electrode was used with lithium metal as both the counter and reference electrodes. The voltage was swept at a scan rate of 1.0 mV s<sup>-1</sup>. Electrochemical measurements of the gel polymer electrolyte were conducted using 2032 coin cells consisting of a separator, Li metal and a LiFePO<sub>4</sub> cathode (90 wt% LiFePO<sub>4</sub>, 5 wt% carbon black, 5 wt% PVDF). All the cells were assembled in argon-charged glove box. After fabrication, the cells with pre-gel solution were subjected to thermal cross-linking for 3 h at 70 °C. The galvanostatic charge–discharge experiments were carried out with voltage range of 2.5–4.2 V using a battery cycler (Wonatech, WBCS3000) at 50 °C.

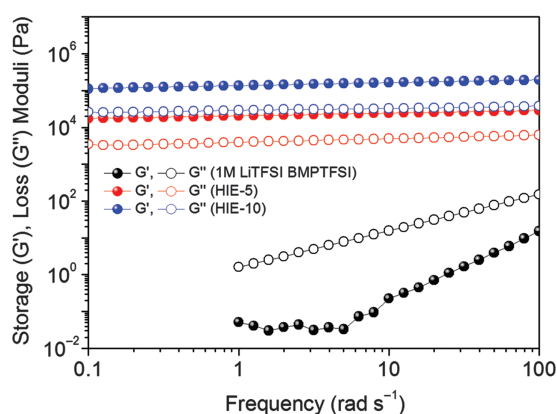
## 3. RESULTS AND DISCUSSION

The inorganic–organic hybrid ionogels were fabricated by thermal initiation of the unsaturated vinyl group of T8-MMA POSS (Fig. 1). After curing process, a mechanically stable and opaque ionogel was obtained. The FT-IR analysis was carried out to characterize the chemical structures of the cured ionogels. As presented in Figure 2, the characteristic peak centered at 1640 cm<sup>-1</sup> derived from the C=C stretching mode of the vinyl group disappeared after thermal treatment, indicating the crosslinking reaction was complete.

Gel formation was further confirmed by observing rheological response before and after thermal curing process.



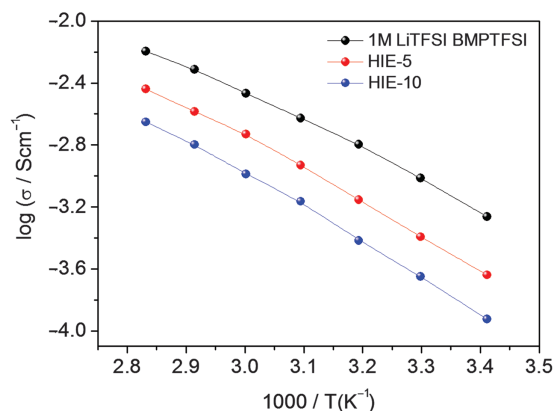
**Figure 2.** FTIR of HIE-5 before and after thermal treatment with inset photographs of the pre-gel hybrid ionogel electrolyte solution and hybrid ionogel electrolyte.



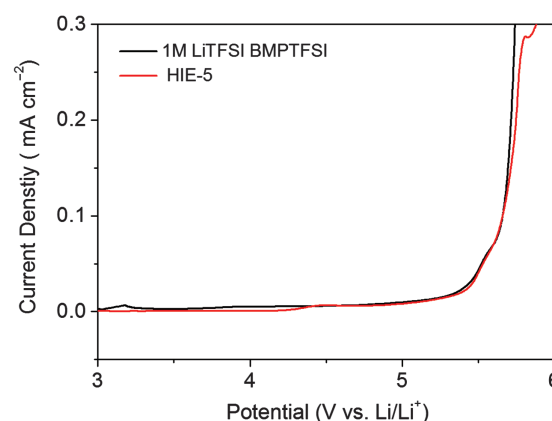
**Figure 3.** Rheological properties of the neat ionic liquid and hybrid ionogel electrolytes.

Figure 3 shows the dynamic viscoelastic properties of neat ionic liquid and hybrid ionogels as a function of the angular frequency. For neat ionic liquid, the loss modulus  $G''$  was found to be greater than storage modulus  $G'$ , and both dynamic moduli values exhibited frequency dependence,  $G' \sim \omega^2$  and  $G'' \sim \omega$ , confirmed a viscous fluid. In contrast, hybrid ionogels fabricated with HIE-5 exhibited a pronounced plateau region of  $G'$  was observed and  $G' > G''$ , demonstrating predominantly solid-like behavior due to the formation of crosslinked network structure. Meanwhile, with further increase in POSS crosslinker content, the network structure was found to be increasingly dense, which was supported by the increase in mechanical properties.

The ionic conductivity of the hybrid ionogels also depended on their network structures. Figure 4 presents the measured ionic conductivity as a function of temperature. All samples exhibited qualitatively similar Arrhenius increases in ionic conductivity with increasing temperature, suggesting the ion conduction was mainly governed by the mobility of free ions. Simultaneously, it is apparent that the gelation of ionic liquid resulted in the decrease in ionic conductivity because the formation of a



**Figure 4.** Temperature dependent ionic conductivities of the neat ionic liquid and hybrid ionogels electrolytes.



**Figure 5.** Linear sweep voltammograms for the ionic liquid and HIE-5.

network structure that restricts the mobility of the ions. However, we were able to solidify ionic liquid solution using only a small amount of gelator ( $\sim 5$  wt%), leading to mitigate the decrease in ionic mobility. The ionic conductivity of HIE-5 was observed to be  $0.51 \text{ mS cm}^{-1}$  at  $30 \text{ }^\circ\text{C}$ , which was close to that of the neat ionic liquid solution.<sup>11</sup>

Before evaluating the electrochemical performances, we investigated the electrochemical stability of ionogels by using linear sweep voltammetry (LSV) measurements. As shown in Figure 5, in the anodic region, LSV profiles of both the neat ionic liquid and hybrid ionogels were found to be almost identical and stable up to  $5.0 \text{ V}$  (V vs.  $\text{Li/Li}^+$ ), indicating that the incorporation of crosslinkable groups into the ionogels does not give rise to any adverse effect on the electrochemical stability of the system. Furthermore, as Figure 6 reveals, the initial weight loss occurred at temperature above  $350 \text{ }^\circ\text{C}$ , indicating the excellent thermal stability of the hybrid ionogels.

To characterize the electrochemical performance of the ionogels,  $\text{LiFePO}_4/\text{HIE-5}/\text{lithium}$  cells were fabricated, and the charge–discharge capacities at various C-rates were investigated at  $50 \text{ }^\circ\text{C}$ . Figure 7 presents the rate capabilities of the cell with hybrid ionogel electrolyte.

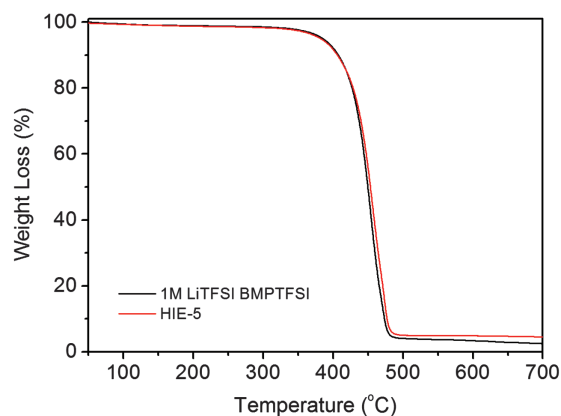


**Figure 6.** TGA thermograms for the ionic liquid and HIE-5.

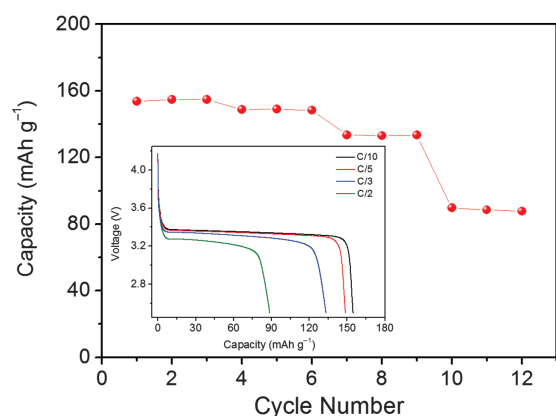


**Figure 7.** Rate capabilities of LiFePO<sub>4</sub>/HIE-5/lithium cells with inset showing the various charge–discharge profile at corresponding C-rates.

For the test, the cell was charged at a current density of 0.1 C and discharged at different current densities. As shown, we were able to achieve stable discharge capacity upon repeated cycling, and the initial discharge capacity of the cell was  $\sim 154 \text{ mAh g}^{-1}$ , which is in close proximity to the theoretical discharge capacity of the LiFePO<sub>4</sub> cathode material.<sup>13</sup> Moreover, the charge and discharge profile exhibited a well-defined potential plateaus, indicating a reversible cycling process. In the following cycles, the discharge capacity and plateau continuously declined with increasing the current densities due to the increase in cell polarization. The cell delivered a moderate discharge capacity of  $88 \text{ mAh g}^{-1}$  at 0.5 C, which was 57% of the discharge capacity of 0.1 C.

Finally, we assessed the cycling performance of the cell through measuring the discharge capacities shown in Figure 8, where the cells were charged at a current density of 0.1 C and discharged at 0.1 C. It can be seen that the discharge capacity of the cell with ionogel was maintained almost stably over 50 cycles. After cycling, the discharge capacity was sustained 86% of its largest value and the Coulombic efficiency of the system was observed

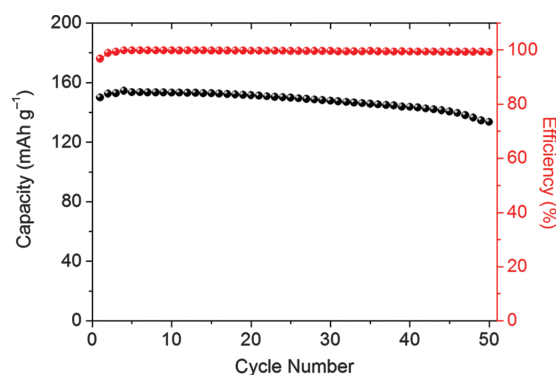


**Figure 8.** Cyclability of LiFePO<sub>4</sub>/HIE-5/lithium cells.

to be above 96% during cycles, demonstrating that these hybrid ionogel electrolytes could be promising candidate electrolyte for use in lithium batteries.

#### 4. CONCLUSION

Fully solution-processable organic–inorganic hybrid ionogel electrolytes were fabricated with a crosslinkable methacrylate-substituted polyhedral oligomeric silsesquioxane with nano-sized inorganic core. Through use of mere 5 wt% of the polyhedral oligomeric silsesquioxane crosslinker, hybrid ionogel electrolytes with high ionic conductivity, high electrochemical stability, thermal stability, and mechanical robustness were prepared. Through evaluation of the lithium ion battery tests, fabricated hybrid ionogel electrolytes exhibited promising performance for next generation electrochemical devices.

**Acknowledgment:** This work was financially supported by a grant from the Fundamental R&D Program for Core Technology of Materials and the Industrial Strategic Technology Development Program funded by the Ministry of Knowledge Economy, Republic of Korea. Partial funding was given by the Materials Architecting Research Center of Korea Institute of Science and Technology and the Korea Research Fellowship Program funded by the Ministry of Science, ICT, and Future Planning through the National Research Foundation of Korea.

#### References and Notes

1. Y. Lu, K. Korf, Y. Kambe, Z. Tu, and L. A. Archer, *Angew. Chem. Int. Ed.* 53, 488 (2014).
2. N. Boarett, A. Bittner, C. Brinkmann, B.-E. Olsowski, J. Schulz, M. Seyfried, K. Vezzu, M. Popall, and V. D. Noto, *Chem. Mater.* 26, 6339 (2014).
3. A. Guyomard-Lack, J. Abusleme, P. Soudan, B. Lestriez, D. Guyomard, and J. L. Bideau, *Adv. Energy Mater.* 4, 1301570 (2014).
4. J. L. Bideau, L. Viaw, and A. Vioux, *Chem. Soc. Rev.* 40, 907 (2011).
5. D. B. Cordes, P. D. Lickiss, and F. Rataboul, *Chem. Rev.* 110, 2081 (2010).
6. J. Choi, S. G. Yoo, and R. M. Laine, *Macromolecules* 37, 99 (2004).
7. Y. Wang, F. Liu, and X. Xue, *Prog. Org. Coat.* 76, 863 (2013).
8. S.-K. Kim, D.-G. Kim, A. Lee, H.-S. Sohn, J. J. Wie, N. A. Nguyen, M. E. Mackay, and J.-C. Lee, *Macromolecules* 45, 9356 (2012).
9. D.-G. Kim, J. Shim, J. H. Lee, S.-J. Kwon, J.-H. Baik, and J.-C. Lee, *Polymer* 54, 5812 (2013).
10. Z. B. Zhou, H. Matsumoto, and K. Tatsumi, *Chem.-Eur. J.* 12, 2196 (2006).
11. J. H. Lee, A. S. Lee, J.-C. Lee, S. M. Hong, S. S. Hwang, and C. M. Koo, *J. Mater. Chem. A* 3, 2226 (2015).
12. A. S. Lee, J. H. Lee, J.-C. Lee, S. M. Hong, S. S. Hwang, and C. M. Koo, *J. Mater. Chem. A* 2, 1277 (2014).
13. M. Wetjen, M. A. Navarra, S. Panero, S. Passerini, B. Scrosati, and J. Hassoun, *ChemSusChem.* 6, 1037 (2013).

Received: 14 November 2015. Accepted: 26 August 2016.